agronomy

MDPI

Article

Effects of Phosphorus Ensembled Nanomaterials on Nutrient Uptake and Distribution in *Glycine max* L. under Simulated Precipitation

Qingqing Li [1,2], Chuanxin Ma [3,4,*], Jason C. White [3] and Baoshan Xing [1,*]

1 Stockbridge School of Agriculture, University of Massachusetts, Amherst, MA 01003, USA; liqq177@gmail.com
2 Zhejiang Provincial Key Laboratory of Organic Pollution Process and Control, Department of Environmental Science, Zhejiang University, Hangzhou 310058, China
3 Connecticut Agricultural Experiment Station, New Haven, CT 06504, USA; Jason.White@ct.gov
4 Laboratory for City Cluster Environmental Safety and Green Development of the Ministry of Education, Institute of Environmental and Ecological Engineering, Guangdong University of Technology, Guangzhou 510006, China
* Correspondence: chuanxin.ma@gdut.edu.cn (C.M.); bx@umass.edu (B.X.)

Abstract: Nanoscale hydroxyapatite (nHA) was synthesized to investigate its potential as a phosphorus (P) ensembled nanofertilizer, using soybean (*Glycine max* L.) as a model plant. The conventional analogue phosphate (pi) was used for comparison with the synthesized nHA. Varied precipitation intensities (0%, 30%, 60%, and 100%) were simulated by adding selected volumes of the P fertilizers (nHA or pi) via foliar spray and soil amendment. The total amounts of added P were the same across all the treatments. The importance of a wash-off effect was investigated on foliar-treated seedlings by evaluating different watering heights (20, 120, and 240 cm above the seedlings). Fresh weight, pigment content, macro-, and micronutrient contents were measured in soybean tissues across all the treatments after 4 weeks of greenhouse cultivation. The synthesized nHA showed superior effects on plant nutrient content upon high precipitation intensities. For example, at 100% precipitation intensity, there was 32.6% more P and 33.2% more Ca in shoots, 40.6% more P and 45.4% more Ca in roots, and 37.9% more P and 82.3% more Ca in pods, as compared to those with pi treatment, respectively. No impact on soybean biomass was evident upon the application of nHA or pi. Further investigation into customizing nHA to enhance its affinity with crop leaves and to extend retention time on the leaf surface is warranted given that the present study did not show significant positive impacts of nHA on soybean growth under the effects of precipitation. Taken together, our findings increase understanding of the potential application of nHA as a nano-enabled fertilizer in sustainable agriculture.

Keywords: nanoscale hydroxyapatite; nutrient; chlorophyll; simulated precipitation; *Glycine max* L.

check for updates

Citation: Li, Q.; Ma, C.; White, J.C.; Xing, B. Effects of Phosphorus Ensembled Nanomaterials on Nutrient Uptake and Distribution in *Glycine max* L. under Simulated Precipitation. *Agronomy* **2021**, *11*, 1086. https://doi.org/10.3390/agronomy11061086

Academic Editors: Sanghamitra Majumdar and Luca Pagano

Received: 20 April 2021
Accepted: 25 May 2021
Published: 27 May 2021

Publisher's Note: MDPI stays neutral with regard to jurisdictional claims in published maps and institutional affiliations.

Copyright: © 2021 by the authors. Licensee MDPI, Basel, Switzerland. This article is an open access article distributed under the terms and conditions of the Creative Commons Attribution (CC BY) license (https://creativecommons.org/licenses/by/4.0/).

1. Introduction

The ability to provide adequate and nutritional food worldwide will be challenged by the rapidly increasing global population, declining arable land, changing climate, and degradation of environmental resources [1–3]. The intensive application of chemical fertilizers has been a common and effective strategy in agriculture for decades [4,5]. However, fertilizer and pesticide efficiency of delivery and utilization is quite low, and as such, they have often been applied excessively to meet crop demands [6–8]. Importantly, over application of these agrochemicals has direct negative environmental consequences, such as toxicity to non-target species, contamination of soil and water, as well as disturbance to the plant diversity [9–12]. For example, the nutrient use efficiency of phosphorus is only 5–30%, and excessively applied amounts run-off into water bodies, serving as a primary driver of eutrophication and dangerous algal blooms [13–15]. Phosphorus has the added

complication of being a finite resource, with declining sources of phosphorus rocks becoming an increasing concern [16–19]. Consequently, the environmental footprint of food production has become both massive and unsustainable. Given the challenges noted above, novel approaches and technologies to sustainably increase agricultural productivity are desperately needed [20–23].

There has been significant growing interest in the use of nanotechnology to enhance crop growth and agricultural production [24–26]. Potential applications of engineered nanomaterials in agriculture include, but are not limited to, nanofertilizers [8,27,28], nanopesticides [8,29], nano-enabled agrochemical carriers [30,31] and nanosensors [32–34]. Selected engineered nanomaterials have been applied as soil amendments, seed coatings, and foliar sprays [35,36]. To meet the goal of controlled release and delivery of active ingredients with reasonable environmental cost and energy input, nanomaterials need to be carefully designed and applied by sustainable methods [23,35,37]. For nanomaterials applied as fertilizers, there has been work on both nanoscale macro- [38–41] and micronutrients [42–45]. Importantly, material properties such as size, morphology, composition, and surface characterization all can be tuned to control release, accumulation, and translocation of nutrients in plants [46–51]. The benefits of using properly-controlled nanomaterials as fertilizers extends not only to precise and accurate delivery, but also to alleviating the negative environmental consequences derived from overapplication and run-off [27,52]. Given its extensive use in biomedical applications, nanoscale hydroxyapatite (nHA) has garnered significant interest as a potential phosphorus fertilizer [53,54]. The synthesis of rod-like hydroxyapatites can be readily achieved through one-step wet chemistry precipitation [55–57]. The synthesized nHA has shown positive effects on soybean, leading to 32.6% and 20.4% increases in growth rate and seed yield, respectively [38]. Exposure to 150 mg P/kg nHA with a negative charge increased sunflower biomass by twofold relative to plants treated with the same amounts of P in the conventional form of triple superphosphate [58]. Recently, nHA has been incorporated into a range of nanocomposites to achieve multifunctionality [40,59,60]. For example, hydroxyapatite-based nanostructured P fertilizers were achieved through an alkali-enhanced hydrothermal process; these materials exhibited significantly elevated phosphorus use efficiency (PUE) of 45.87% and 46.21% from two different precursors ($CaHPO_4$ and CaP_2O_7) as compared to a chemical P fertilizer with a PUE of 23.44% [40]. Similarly, soil amendment of nHA functionalized with humic substances significantly improved early *Zea mays* growth, productivity, rhizosphere bacteria diversity, and tolerance to NaCl-induced abiotic stresses [60].

In the current study, nHA was synthesized using a wet chemistry precipitation method. The nanoscale fertilizer was applied to soybean foliage and roots simultaneously to simulate different precipitation intensities; comparisons to equivalent conventional bulk amendments were included. Additionally, the foliar retention ability of the synthesized nanofertilizer was evaluated through a wash-off test in which precipitation intensities were controlled at different watering heights (20–240 cm). The present study provides valuable information on the efficacy of nanoscale P materials as a component of sustainable nano-enabled agricultural practices. Moreover, discussion on the costs and benefits of both nanoscale and conventional fertilizers through the two application methods provides insight into the rational design of smart agrochemicals.

2. Experimental Section

2.1. Synthesis and Characterization of Hydroxyapatite Nanoparticles

Hydroxyapatite nanoparticles (nHA) were synthesized using a wet chemistry precipitation method by mixing calcium (II) and phosphate (1.67:1, mole weight ratio) in an alkaline solution under controlled temperatures (80 °C). Briefly, 40 mL of 1.0 M $Ca(NO_3)_2$ solution was incubated in an water bath with continuous stirring. Then, 40 mL of 0.6 M NaH_2PO_4 aqueous solution was added drop-wise into the cold Ca $(NO_3)_2$ solution. The solution pH was adjusted to approximately 12.0 by adding 2.0 M NaOH, and the solution was continuously stirred for 24 h. The resulting white precipitate was washed with

deionized (DI) water to remove extraneous salts and alkaline materials. The solution was freeze dried to enable recovery of the hydroxyapatite nanoparticles. The resulting white precipitates were observed by transmission electron microscopy (TEM, JEOL JEM-2000FX, Tokyo, Japan), and functional group characterization was evaluated by Fourier Transform Infrared Spectroscopy (FT-IR spectrometer, PerkinElmer Spectrum, Waltham, MA, USA).

2.2. Greenhouse Cultivation

Soybean seeds were germinated in a mixture of vermiculite and PRO-MIX (1:3, *v*/*v*), and then seedlings were transplanted into soil (300 g/pot) after the two unifoliate leaves were fully developed. The soil was collected from the Crop and Animal Research and Education Farm at the University of Massachusetts, Amherst. Five replicate pots were used for each treatment. Plants were watered daily with 50 mL tap water through the trays under the pods. The greenhouse temperature was set at 22 °C for 16 h during the day and 18 °C for 8 h at night. Soybean seedlings were treated with nHA (P-nanofertilizer) or dicalcium phosphate (pi) through foliage (foliar spray) and root pathways (soil amendment) once per week over a 28-day growth period. The equivalent molar concentration of phosphorus (0.7 mmol/L) was used for both nHA and pi.

2.3. Simulated Precipitation Experiment

In order to simulate different precipitation intensities (0%, 30%, 60%, and 100%), 4 mL of prepared P-nanofertilizer or pi was sprayed onto the leaves and amended into the soil simultaneously. For the foliar spray, soil in the pots was covered with paper towels to avoid spraying onto the soil. For soil amendment, P-nanofertilizer or pi was pipetted through three pre-inserted tips. The pipette tips were inserted into soil (1 cm underneath) around the seedlings with equal distances. Detailed information for each treatment is listed in Table 1; *A*, *B*, *C*, and *D* are treatments with nHA, and *A′*, *B′*, *C′*, and *D′* are treatments with pi, respectively. The simulated precipitation experiment was schematically illustrated in Figure 1A.

Table 1. Details of each treatment in the simulated precipitation experiment.

Label	Treatment Details
Control (CK)	4 mL water sprayed onto foliage
A (0%)	4 mL nHA (0.7 mmol/L) sprayed onto foliage
B (30%)	2.8 mL nHA (0.7 mmol/L) sprayed onto foliage, and 1.2 mL nHA (0.7 mmol/L) added into soil
C (60%)	1.6 mL nHA (0.7 mmol/L) sprayed onto foliage, and 2.4 mL nHA (0.7 mmol/L) added into soil
D (100%)	4 mL nHA (0.7 mmol/L) added into soil
A′ (0%)	4 mL pi (0.7 mmol/L) sprayed onto foliage
B′ (30%)	2.8 mL pi (0.7 mmol/L) sprayed onto foliage, and 1.2 mL pi (0.7 mmol/L) added into soil
C′ (60%)	1.6 mL pi (0.7 mmol/L) sprayed onto foliage, and 2.4 mL pi (0.7 mmol/L) added into soil
D′ (100%)	4 mL water sprayed onto foliage

2.4. Wash-Off Test from Different Heights

In order to evaluate leaching upon precipitation, a separate experiment with varied precipitation heights (20 cm, 120 cm, and 240 cm) was conducted. A wash-off test was conducted one day prior to the next round of P fertilizer application. Five hundred millilitres of tap water was applied to each pot over the course of the experiment. Details of these treatments are listed in Table 2, in which *E*, *F*, and *G* represent the wash-off tests with nHA, and *E′*, *F′*, and *G′* represent the wash-off tests with pi. *A* and *A′* from the simulated precipitation experiment were used as no wash-off controls, respectively. The wash-off test is schematically illustrated in Figure 1B.

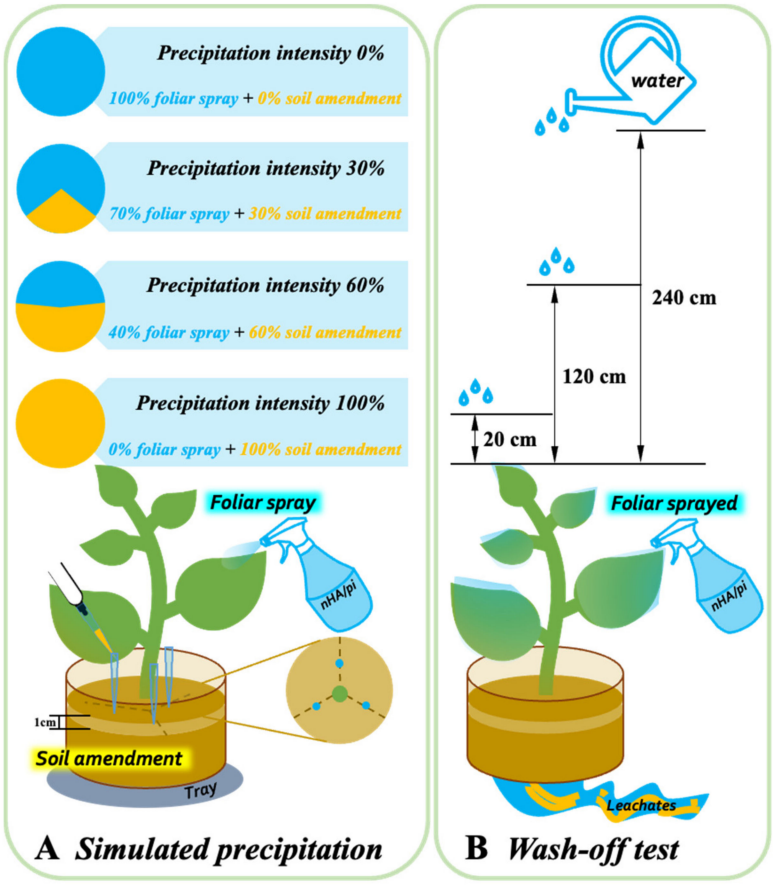


Figure 1. Schematic illustrations of simulated precipitation (**A**) and wash-off test (**B**).

Table 2. Details of each treatment in the wash-off test.

Label	Treatment Details
Control (CK)	4 mL water sprayed onto foliage
A (no wash-off)	4 mL nHA (0.7 mmol/L) sprayed onto foliage
A′ (no wash-off)	4 mL pi (0.7 mmol/L) sprayed onto foliage
E (20 cm)	*A* with precipitation from 20 cm above seedlings
F (120 cm)	*A* with precipitation from 120 cm above seedlings
G (240 cm)	*A* with precipitation from 240 cm above seedlings
E′ (20 cm)	*A′* with precipitation from 20 cm above seedlings
F′ (120 cm)	*A′* with precipitation from 120 cm above seedlings
G′ (240 cm)	*A′* with precipitation from 240 cm above seedlings

2.5. Plant Harvest

At harvest, soybean seedlings were washed with tap water, followed by deionized water rinsing three times. Intact leaves were washed with 1 mM HNO_3 and rinsed by ice cold 2 mM $CaCl_2$ and DI water to separate unabsorbed NPs from the leaves [61–63]. The fresh biomass of shoots and roots were separately weighed across all the treatments. Fresh shoots, roots, and pods were collected for pigment and elemental analysis.

2.5.1. Pigment Measurement

The chlorophyll and carotenoid content of soybean leaves were measured across all the treatments according to Lichtenthaler et al. (2001) [64]. Approximately 50 mg of fresh leaves were cut into small pieces and then extracted in 3 mL of 95% (*v*/*v*) ethanol. The samples were kept in the dark for 72 h prior to measurement. Absorbances at 470, 664.2, and 648.6 nm were recorded using a UV-Vis spectrophotometer (Cary 60 UV Vis; Agilent Technologies). The content of chlorophyll *a*, *b*, total chlorophyll, and carotenoid content

were calculated using the following equations: c_a (Chl *a*, μg/mL) = $13.36A_{664.2} - 5.19A_{648.6}$; c_b (Chl *b*, μg/mL) = $27.43A_{648.6} - 8.12A_{664.2}$; c_{a+b} (Total Chl, μg/mL) = $c_a + c_b = 5.24A_{664.2} + 22.24A_{648.6}$; $c_{(x+c)}$ (Carotenoids, μg/mL) = $(1000A_{470} - 2.13c_a - 97.64c_b)/209$.

2.5.2. Elemental Analysis in Plant Tissues

Approximately 100–400 mg of fresh tissues of pods, roots, or shoots of soybean were cut into pieces and transferred in vials, followed by freeze-drying in a lyophilizer (Free Zone 2.5 Liter-50C; Labcon co, Kansas, MI, USA) for 72 h. The mass difference between the fresh biomass and dry biomass was used to calculate water content. Freeze-dried tissues were ground into fine powder, and then approximately 50 mg of dry tissues were transferred into a digestion tube containing 3 mL of concentrated HNO_3. The samples were pre-digested at the ambient temperature overnight. Then, the pre-digesta were heated at 105 °C on a hot block (DigiPREP System; SCP Science, Baie-d'Urfé, QC, Canada) for 40 min; after the digesta cooled to an ambient temperature, 500 μL of H_2O_2 was then added prior to heating at 105 °C for an additional 20 min to complete the digestion. A volume of 300 μL of digesta was diluted to 30 mL with DI water prior to elemental analysis. The content of macro- (P, K, Ca, Mg, and S) and micronutrients (Cu, Zn, Mn, and Fe) was determined by inductively coupled plasma optical emission spectrometry (ICP-OES, iCAP 6500; Thermo Fisher Scientific, Waltham, MA, USA).

2.5.3. Statistical Analysis

Each treatment contained four or five replicates. All soybean pots were randomly arranged on greenhouse benches and rearranged on a weekly basis. SPSS statistics software (version 26, IBM Corp, Endicott, NY, USA) was used for the significance analysis. Two sets of one-way analyses of variance (one-yay ANOVA) followed by Waller–Duncan multiple comparison were used to perform statistical analyses for treatments in the simulated precipitation experiment and wash-off test separately. In figures and tables, values of each assay that are followed by different letters are significantly different at $p < 0.05$.

3. Results and Discussion

3.1. Characterization of the Synthesized Nano-Hydroxyapatites

Nanoscale HA particles exhibited a needle-like shape with dimensions of approximately 20 nm in diameter and 100–200 nm in length (Figure 2A). In the FTIR spectrum (Figure 2B), OH- bands appeared at around 3400 cm^{-1}. Bands that appeared at 1023 and 962 cm^{-1} represent asymmetrical and symmetrical stretching of P-O bond of the PO_4^{3}, respectively; the peak at 860 cm^{-1} corresponds to the symmetrical stretching mode of the P−O(H) bond of the HPO_2^{4-} group [65,66]. The band at 1414 cm^{-1} indicates the presence of carbonate groups.

3.2. Physiological Responses of nHA- and pi-Treated Soybean under Simulated Precipitation and Wash-Off Conditions

As shown in Figure 3A,B and Figure S1A, externally applied P fertilizers had a slight but statistically insignificant enhancing effect on soybean biomass over the 28 days of treatment; differences between the nHA and pi treatments at the same precipitation intensities were not significant. This result is consist with the previous report by Liu and Lal, in which synthetic apatite nanoparticles only slightly improved soybean growth (biomass) relative to triple-phosphate [38]. In the wash-off test, the fresh biomass of nHA- and pi-treated soybean were significantly decreased (Figure S3) as compared to the control. Specifically, the root biomass of nHA- and pi-treated soybean was decreased by up to 27.6% and 21.0%, respectively, as compared to the control. A reasonable explanation for this effect could be the loss of surface-applied P fertilizer and successive leaching of nutrients from the soil. Foliar spray of the P fertilizers and subsequent wash-off could potentially cause phyllosphere dysbiosis and a subsequent decrease in crop biomass. It is also known that rain and/or high air humidity can induce phyllosphere dysbiosis and disease outbreaks

in plants [67–69], which could potentially impede seedling growth and development. In addition, in comparison with foliar spray, soil irrigation could result in soil compaction and inhibition of root respiration [70], both of which could negatively affect plant health.

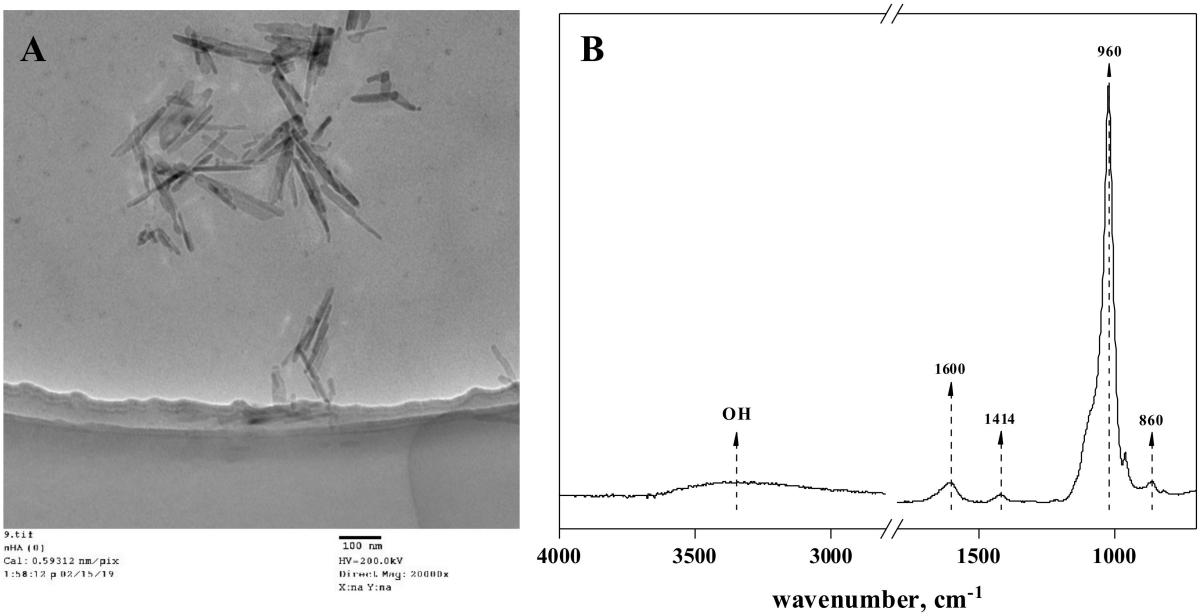


Figure 2. Characterization of the synthesized nHA: (**A**) TEM image (scale bar 100 nm), and (**B**) FTIR spectrum.

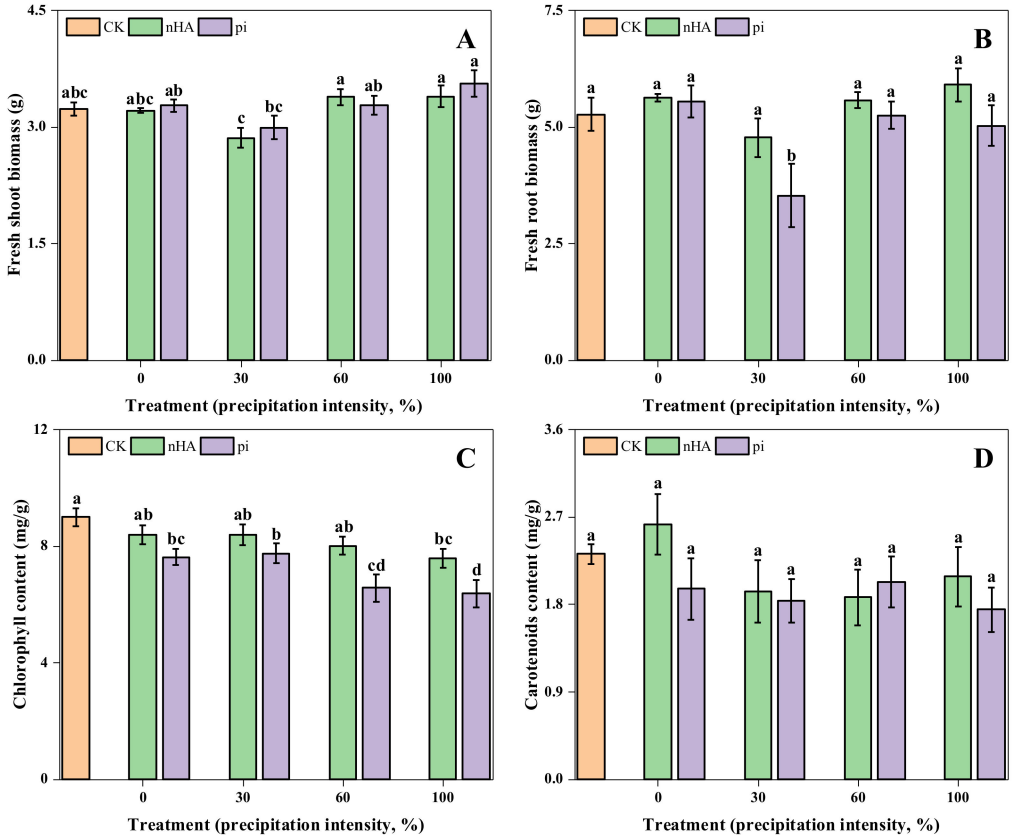


Figure 3. Physiological effects of foliar- and soil-applied nHA or pi on the growth of treated soybean (under a simulated precipitation scenario): (**A**) fresh shoot biomass, (**B**) fresh root biomass, (**C**) chlorophyll content, and (**D**) carotenoids content. Error bars correspond to standard errors of the means. Values of fresh biomass, chlorophyll, and carotenoid content that are followed by different letters are significantly different at $p < 0.05$.

Pigment content is an important parameter for evaluating plant photosynthesis under a range of treatment conditions [71,72]. Leaf chlorophyll content was less than the untreated group under all pi treatments, and it decreased further along with increases in the precipitation intensity. For example, compared to the control, at 0% precipitation intensity, chlorophyll content decreased by 15.3% in pi-treated soybean shoots; at 100% precipitation intensity, chlorophyll contents decreased by 15.7% and 29.2% in nHA- and pi-treated shoots, respectively (Figure 3C). Reduction effect on the chlorophyll content with pi treatments was stronger than those with nHA treatment under the same precipitation intensity. Specifically, as shown in Figure S1B,C, the slight decrease in chlorophyll contents in nHA-treated soybean shoots was primarily due to the reduction in the chlorophyll *a* content. A similar trend of decreasing chlorophyll content along with the increasing of precipitation intensity was also evident in the wash-off test (Figure S3F). In this case, the decrease of chlorophyll content was mostly ascribed to the decrease of chlorophyll *b* levels. For example, at a precipitation height of 240 cm, the chlorophyll *b* content in nHA- and pi-treated shoots decreased by 38.3 and 45.1%, respectively (Figure S3E). Externally applied nHA and pi had no effects on carotenoid contents in both simulated precipitation and wash-off treated plants. It was reported that chlorophyll *a* content could be used as an indicator for abiotic stress [71,73,74]. At this point, there seemed to be no positive impact and some potentially negative impacts of external P fertilizers on the soybean photosynthesis.

3.3. Nutrient Contents in Soybean

3.3.1. Macronutrient Contents in Shoots, Roots, and Soil

The macronutrient content in soybean shoots, roots, and soil treated by nHA and pi in the simulated precipitation scenario are shown in Figures 4 and 5 and Figure S2. At 0% precipitation intensity, when all the external P fertilizers were applied through foliage, pi treatment resulted in a 36.9% increase in shoot P contents and a 26.8% increase in root P compared to the untreated group. Conversely, once all the external P fertilizers were amended into soil (100% precipitation intensity), nHA treatment had significantly enhanced P accumulation in the seedlings, while pi showed no effect with statistical difference. For example, the shoot and root P content in the nHA-treated soybeans at 100% precipitation intensity was 44.0% and 24.0% higher than the control, respectively (Figure 4A,B). Calcium is an important structural element regulating cell wall stability and membrane permeability [75,76] and is another primary component of nHA and pi. Correspondingly, at 0% precipitation intensity, pi-treated soybean seedlings had 79.8% more Ca in shoots and 18.6% more Ca in roots compared to the controls, while nHA-treated soybean seedlings had 23.2% more Ca in shoots and no difference between roots and the control. At 100% precipitation intensity, pi-treated seedlings had 28.5% more Ca in the shoots and 20.3% less Ca in the roots compared with unamended ones, while nHA-treated seedlings had 71.1% more Ca in the shoots and 15.9% more Ca in the roots compared to the respective controls, which are statistically higher than those of the pi treatment (Figure 4D,E).

nHA and pi treatments exhibited opposite trends on nutrient content as a function of precipitation intensity, both in shoots and roots. First, this could be a result of greater nHA availability in the soil ascribed to less binding to soil minerals that would form insoluble phosphates [77–79]; this subsequently results in greater P and Ca bioavailability for root-to-shoot transport. Second, plants require P in the phosphate form; thus, when nHA/pi were sprayed onto the foliar surfaces, longer retention time was required for the uptake of nHA than pi. Consequently, nHA may aggregate before uptake by the leaves, which could subsequently undermine P content [80,81].

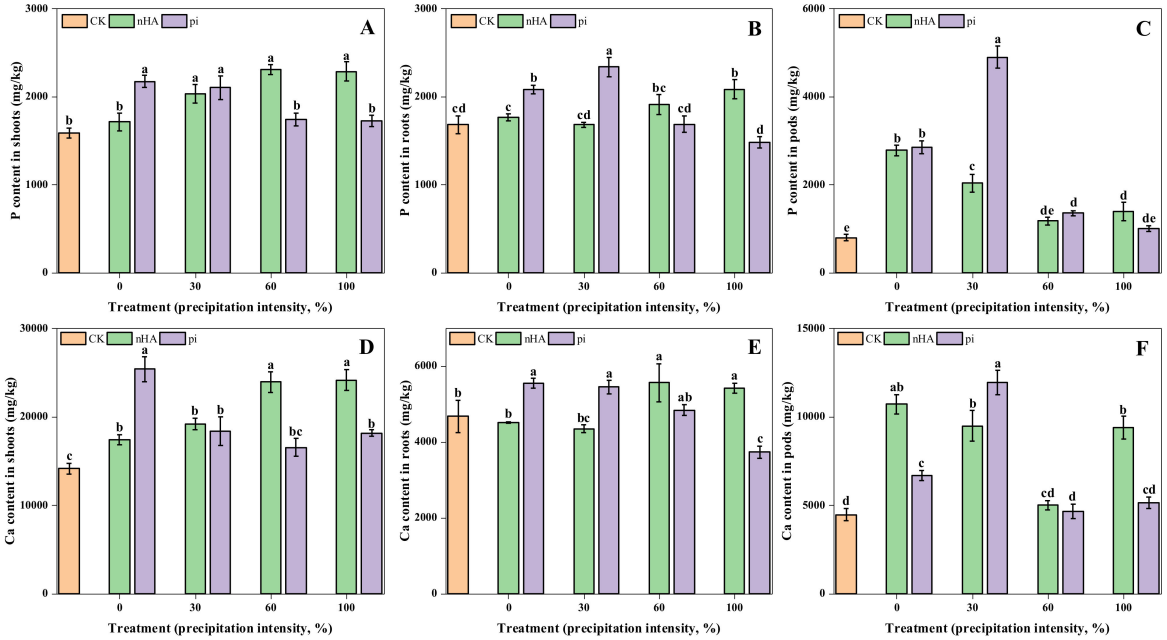


Figure 4. The content of P and Ca in soybean shoots (**A**,**D**, respectively), roots (**B**,**E**, respectively), and pods (**C**,**F**, respectively) treated with nHA or pi (under simulated precipitation scenario). Error bars correspond to the standard errors of the means. Values of each nutrient content that are followed by different letters are significantly different at $p < 0.05$.

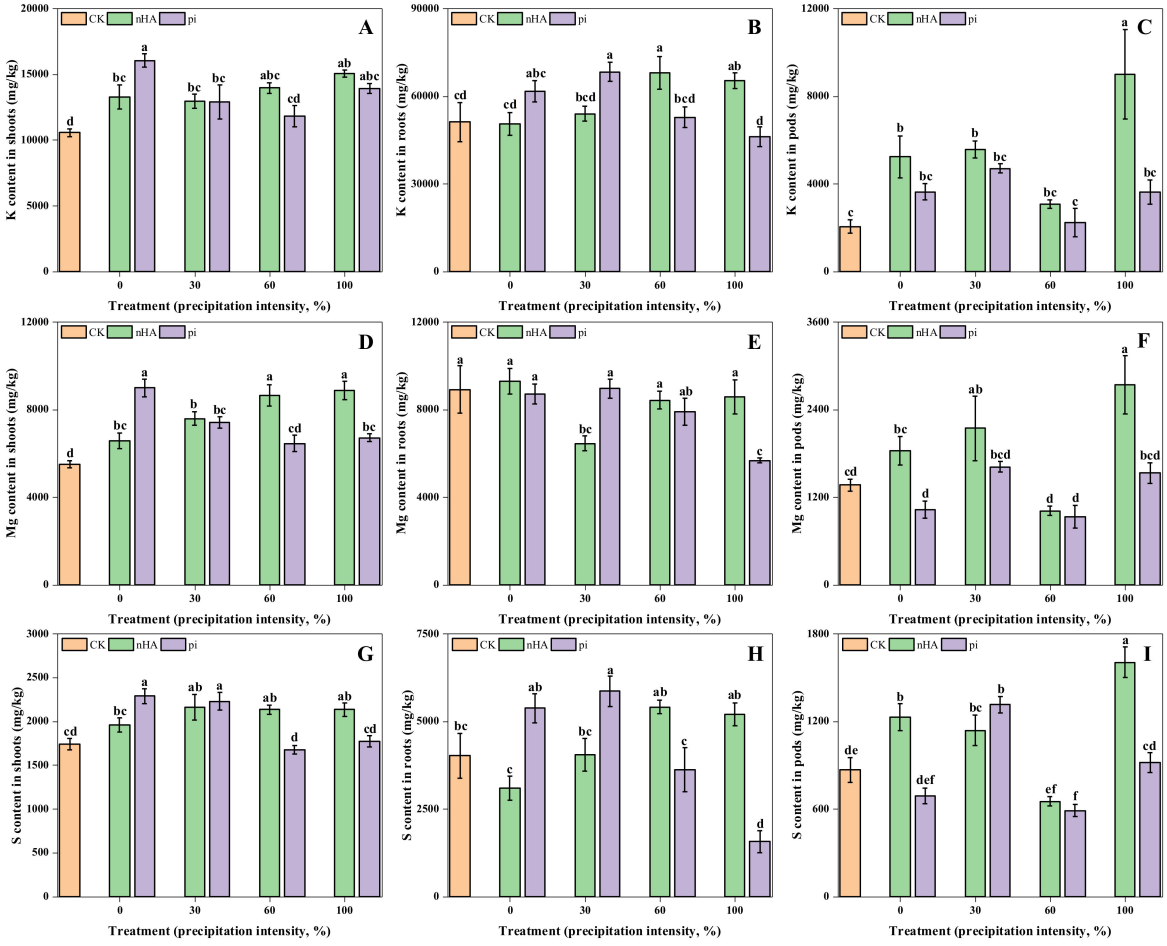


Figure 5. The content of K, Mg, and S in soybean shoots (**A**,**D**,**G**, respectively), roots (**B**,**E**,**H**, respectively), and pods (**C**,**F**,**I**, respectively) treated with nHA or pi (under the simulated precipitation scenario). Error bars correspond to standard errors of the means. Values of each nutrient content that are followed by different letters are significantly different at $p < 0.05$.

Such trends were not limited only to the elements that were externally applied; the macro nutrients K, Mg, and S were increased in shoots and roots with increases in the soil P-nanofertilizer amendment (Figure 5). Since there was no external K, Mg, and S source in the treated groups, the increase of these macronutrients was facilitated by the soil (Figure S2). Although there were no discernible patterns in the variations among the different treatments with different precipitation intensities, nutrients in the soil also contributed to the plant growth upon treatment with the external fertilizers. For example, at 100% precipitation intensity, 10.0% more P, 17.6% more Ca, 14.6% more Mg, and 54.8% more S were depleted from the soil in the nHA treatment compared to the untreated group. The K content in soil was not altered across all the nHA treatments. Since there were trays under each pot, there was no chance of the nutrient loss from the leachates, and since there was no visible leaching observed throughout the whole experiment period, the depleted soil nutrients were all being taken up by the seedlings. The input of external nanoscale P fertilizers to the soil could be regarded as a means to enhance the uptake of other soil nutrients. Therefore, when the P fertilizers were all added to the soil (at 100% precipitation intensity), 42.8% more K, 61.2% more Mg, and 22.7% more S in nHA-treated soybean shoots could be ascribed to root-to-shoot transport, as compared to the control.

For pi-treated soybeans, similar soil nutrient depletion was also evident. At 0% precipitation intensity, 9.7% P, 13.5% Ca, 14.1% Mg, and 28.3% S were depleted from soil and taken up by the seedlings (Figure S2). The K content in soil was not altered across all the pi treatments. In contrast to the nHA treatment, shoot and root macronutrient content decreased with the increase in precipitation intensity (Figures 3B,E and 4B,E,H). At 100% precipitation intensity, the root macronutrient content was notably less than the control (20.3% less Ca, 36.3% less Mg, and 61.1% less S); soil macronutrient content was equivalent with the control except for S, which was reduced by 42.6% compared to the control (Figure S2E). There was no enhancement effect of externally applied conventional fertilizer on the uptake of other soil nutrients from soil due to inevitable loss of elements by soil binding. In addition, there might have been a potential root-to-shoot mobilization, which could have contributed to the accumulation of nutrients in the shoots. However, the growth of the seedlings could have been impeded due to the lack of root–shoot nutritional balance. Further investigation is needed for clarity. Sulfur is essential for pod formation, and its mobilization is critical to the plant's reproductive life cycle [82,83]. Moreover, it has been reported that N and S assimilation could be altered by changes in the P environment; N and S metabolism require rRNA for synthesis, and rRNA is the largest pool of organic P in leaf cells [84,85]. In the current study, the drastic alteration of S content in the plants could have been a response to the P environment change, as well as the development of pods.

In the wash-off test, soybean seedlings treated with nHA and pi responded differently (Figure S4). Soybeans treated with pi accumulated the greatest amount of macronutrients in shoots and roots without wash-off. However, the macronutrient contents in both shoots and roots decreased significantly after wash-off, suggesting that much of the pi had been removed from the leaf surfaces. In addition, there were no statistically significant differences in shoot/root macronutrient content among different wash-off heights. Moreover, the mobilization of soil nutrients to the plants was not evident in the wash-off treated groups, with the exception being S, which was decreased by 25.5% at a wash-off height of 240 cm, as compared to the control (Figure S6). With the treatment of wash-off, more K accumulated in the soil. For example, 24.2% more K accumulated in the soil at a wash-off height 120 cm. For nHA-treated seedlings, wash-off had a different impact. Other than no significant effects at a higher wash-off height (120 and 240 cm), the enhancement effect on the nutrients acquisition in soybean shoots was still evident at the wash-off height of 20 cm. Specifically, 11.9% more P, 37.0% more Ca, 35.5% more K, 41.7% more Mg, and 15.5% more S were accumulated in soybean shoots as compared to the untreated group (Figure S4), which was even better than the no wash-off group.

Overall, nHA and pi could supply equivalent amounts of P and Ca to plants via root and foliar exposures, respectively. Given that complete breakdown of nHA, either on the leaf surface or in the soil, was not evaluated in this study, a longer-term full life cycle study is needed to fully understand the role of nHA in supplying P and Ca to crops. Furthermore, in a realistic environmental scenario, wash-off of the foliar-applied fertilizers is inevitable and is a key factor that lowers the nutrient availability; additional investigations on ways to increase of nutrient use efficiency through the careful design of nanofertilizers are needed.

3.3.2. Micronutrient Contents in Shoots, Roots and Soil

The content of Cu, Zn, Fe, Mn, and B in soybean tissues across all the treatments varied to different extents as compared to the respective controls (Figure 6). Unlike the macronutrients, there were few discernible trends in the soybean tissue micronutrients. For the nHA-treated seedlings, the enhancing effect of nHA application on micronutrient uptake into the shoots/roots was evident at 100% precipitation intensity on select elements. For example, there was 69.7% more Zn and 60.1% more Mn accumulated in nHA-treated soybean shoots, and 76.7% more Cu accumulated in nHA-treated soybean roots, as compared to the control (Figure 6B). For the pi-treated seedlings, the enhancing effect of pi application on micronutrient uptake into the shoots/roots was only evident at 0% precipitation intensity on selected elements. For example, there was 94.7% more Zn, 25.9% more Fe, and 51.1% more Mn that accumulated in pi-treated soybean shoots and 83.7% more Cu in pi-treated roots, as compared to the control. With the increase of the soil pi supply and the corresponding decrease of total available pi to the plants, root micronutrient contents were notably decreased compared to the control. For example, Cu, Zn, Fe, Mn, and B content at 100% precipitation intensity were reduced by 45.3%, 84.4%, 14.7%, 23.9%, and 25.1%, respectively, as compared to the ones at 0% precipitation intensity (Figure 6B). Moreover, Zn, Fe, Mn, and B contents in pi-treated soybean roots were unexpectedly less than the control. The mechanism by which the soil amendment of pi impeded the root accumulation of these micronutrients is unknown. In this case, further investigations optimizing the fertilizer application route, pattern, and techniques are needed.

Similar to the above-mentioned macronutrients that were not externally applied, increased micronutrient contents in the soybean tissues were all due to soil uptake (Figure S2). For example, at 100% precipitation intensity, when nHA/pi was supplied through soil amendment, Cu, Zn, and Fe content in soil were depleted by 18.6%, 18.2%, and 12.5%, respectively, with nHA treatment as compared to the control; while there was no significant alteration with pi treatment. Conversely at 0% precipitation intensity, when nHA/pi was supplied through foliar spray, Cu, Zn, and Fe content in soil were depleted by 15.7%, 16.9%, and 11.1%, respectively, with pi treatment as compared to the control; while there was no significant alteration with nHA treatment. nHA is more suitable for soil amendment to enhance soybean shoot nutrient acquisition, while pi is better for foliar spray. At 0% precipitation intensity, pi-treated seedlings had 15.5% more Cu, 84.0% more Zn, 19.2% more Fe, 52.3% more Mn, and 10.1% more B in shoots than nHA-treated plants; while at 60% precipitation intensity, nHA-treated soybean seedlings had 91.3% more Cu, 137.5% more Zn, 25.5% more Fe, 63.4% more Mn, and 21.2% more B in shoots than pi-treated ones (Figure 6).

In the wash-off test, the enhancement effect of the nHA/pi application on micronutrient uptake into the shoots/roots was gradually lost with increasing of the wash-off height (Figure S5), with the exception being Cu, which showed increased accumulation in soybean roots upon the wash-off.

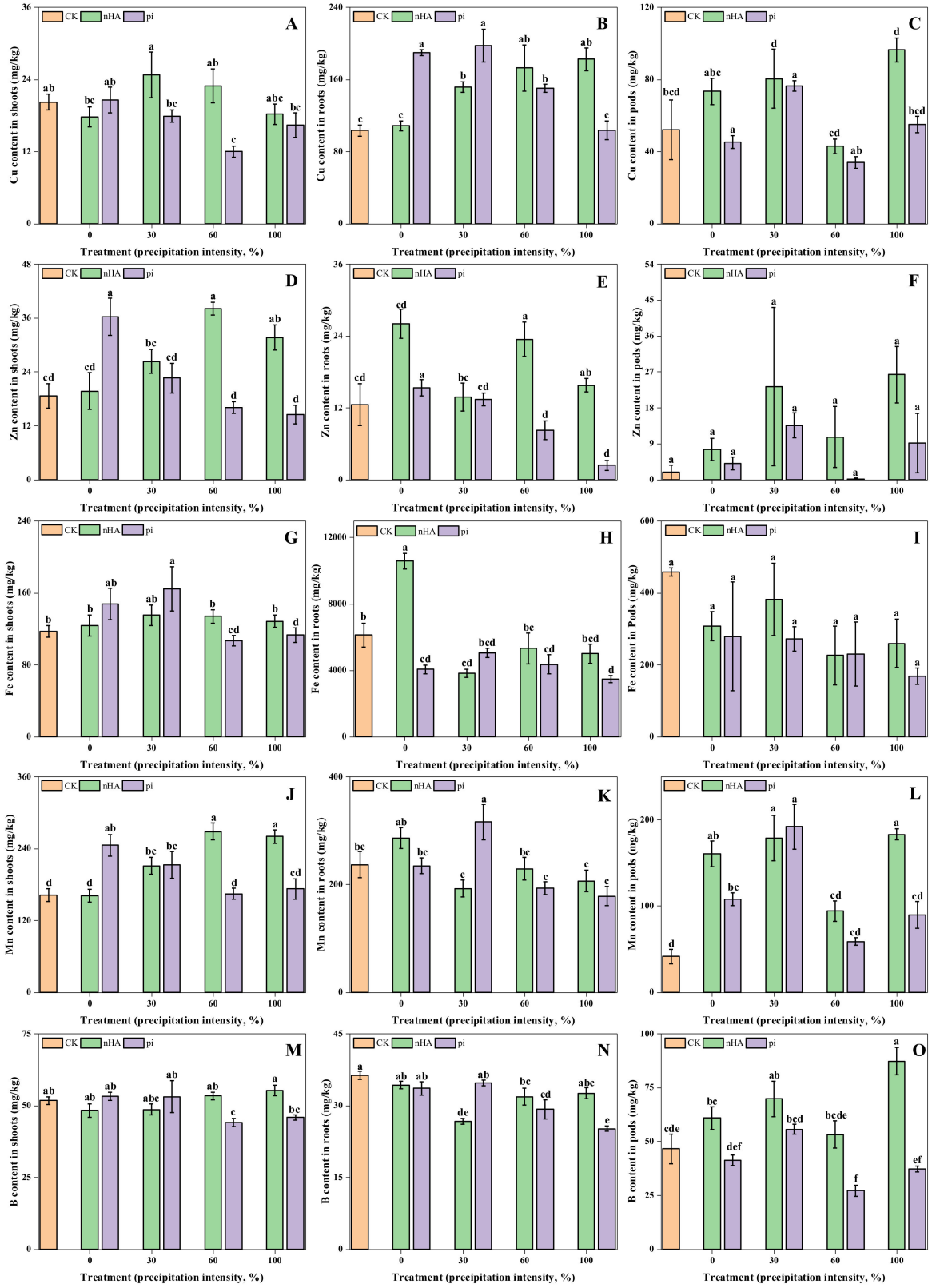


Figure 6. The content of Cu, Zn, Fe, Mn, and B in soybean shoots (**A**,**D**,**G**,**J**,**M**, respectively), roots (**B**,**E**,**H**,**K**,**N**, respectively), and pods (**C**,**F**,**I**,**L**,**O**, respectively) treated with nHA or pi (under the simulated precipitation scenario). Error bars correspond to standard errors of the means. Values of each nutrient content in shoots, roots, and pods that are followed by different letters are significantly different at $p < 0.05$.

3.3.3. Nutrient Contents in Edible Tissues

The content of both micro- and macronutrients in the immature soybean pods were increased upon exposure to both P fertilizers across all treatments (Figures 4C,F, 5C,F,I and 6C,F,I,L,O), although the effects were not dose-dependent. The highest P and Ca accumulation occurred in the nHA treatment with 0% precipitation intensity and the pi treatment with 30% precipitation intensity. nHA-treated soybean pods had 250.6% more P and 140.1% more Ca than the control (Figure 4C, at 0% precipitation intensity), and pi-treated soybean pods had 518.7% more P and 167.7% more Ca than the control (Figure 4F, at 30% precipitation intensity). Upon the application of nHA/pi, the accumulation of other macro/micronutrients in the soybean pods was also stimulated. For example, upon the nHA treatment at 100% precipitation intensity, as compared to the controls, soybean pods had 342.3% more K, 100.7% more Mg, 85.1% more S, 85.3% more Cu, 1387.0% more Zn, 343.2% more Mn, and 87.5% more B; upon the pi treatment at 30% precipitation intensity, soybean pods had 130.8% more K, 51.5% more S, 47.0% more Cu, 667.1% more Zn, and 364.6% more Mn. The enhancing effect of nHA on the nutrients acquisition in the soybean pods was significantly greater than pi across nearly all treatments. The nutrient composition and content in the early stage of pods is highly dynamic, which likely explains the high variability. In addition, it is noteworthy that the reproductive growth period of a crop can be altered upon environmental condition changes, such as P deficiency and warmer temperatures, among others [86,87]. The slow-release property of the externally applied P-nanofertilizer may potentially impact the time required for pod development [88]; this effect needs additional investigation. Regarding the effects of wash-off on the pods, both the macro- and micronutrients content in pods were notably decreased across most of the wash off-treatments, likely due to the loss of nutrients from the leaves (Figures S4 and S5). It is noteworthy that after wash-off, P content in pi-treated soybean pods at wash-off heights of 20 and 120 cm were still equivalent to the plants without wash-off; this could be ascribed to the readily uptake of pi by the above-ground portion of the soybean.

4. Conclusions

This study evaluated the effects of nanoscale and conventional P fertilizers on the development and growth of soybean seedlings. A precipitation intensity variable was incorporated into the experiments, and the costs and benefits of both P fertilizers under foliar and soil application scenarios were evaluated. For foliar spray of the P fertilizers, maintaining high retention on the leaf surface to facilitate direct uptake is important, while for soil amendment, maintaining high bioavailability is the most important. Our findings suggest that a P-nanofertilizer (nHA) could be a better option as a soil amendment compared to a conventional phosphate fertilizer, while pi may be the better option for foliar fertilization. However, encapsulating the nHA into a carrier material, such as a biopolymer, could significantly promote efficacy of the foliar application approach. Importantly, the P-nanofertilizer was superior in stimulating P nutrient accumulation in soybean pods during early development. The findings of this study add to the growing body of literature demonstrating that nanoscale fertilizer strategies may offer increased efficiency of delivery and utilization, while simultaneously alleviating some of the negative impacts associated with agriculture.

Supplementary Materials: The following are available online at https://www.mdpi.com/article/10.3390/agronomy11061086/s1, Physiological effects of simulated precipitation on the growth of treated (Figure S1); Soil nutrient contents under the simulated precipitation scenario (Figure S2); Physiological effects of wash-off on the growth of treated soybeans (Figure S3); Macronutrient contents under the wash-off test (Figure S4); Micronutrient contents under the wash-off test (Figure S5); Soil nutrient contents under wash-off test (Figure S6).

Author Contributions: Conceptualization: Q.L., C.M. and B.X.; data acquisition analysis, and interpretation, Q.L. and C.M.; writing—original draft preparation, Q.L.; writing—review and editing, Q.L., C.M., J.C.W., and B.X. All authors have read and agreed to the published version of the manuscript.

Funding: This research was funded by the National Natural Science Foundation of China (Grant 21707119), the Program for Guangdong Introducing Innovative and Entrepreneurial Teams (2019ZT08L213), and USDA Hatch Program (MAS 00549 and CONH00147).

Institutional Review Board Statement: Not applicable.

Informed Consent Statement: Not applicable.

Data Availability Statement: The data presented in this study are available upon reasonable request from the corresponding author.

Acknowledgments: We acknowledge the CNS Research and Education Greenhouse (UMass Amherst) staff for the technical support with plant cultivation; and the Connecticut Agricultural Experiment Station for the nutrient measurement.

Conflicts of Interest: The authors declare no conflict of interest.

References

1. Alexandratos, N.; Bruinsma, J. *World Agriculture towards 2030/2050: The 2012 Revision*; ESA Working paper No.12-03; FAO: Rome, Italy, 2012.
2. United Nations, Department of Economic and Social Affairs. *World Population Prospects: The 2017 Revision, Key Findings and Advance Tables*; ESA/P/WP/248; United Nations: New York, NY, USA, 2017.
3. United Nations, Department of Economic and Social Affairs. *World Population Prospects 2019: Highlights*; ST/ESA/SER.A/423; United Nations: New York, NY, USA, 2019.
4. Mueller, N.D.; Gerber, J.S.; Johnston, M.; Ray, D.K.; Ramankutty, N.; Foley, J.A. Closing yield gaps through nutrient and water management. *Nature* **2012**, *490*, 254. [CrossRef]
5. FAO. *World Fertilizer Trends and Outlook to 2022*; FAO: Rome, Italy, 2019.
6. FAO. *The State of Food and Agriculture: Moving forward on Food Loss and Waste Reduction*; Food and Agriculture Organization of the United Nations: Rome, Italy, 2019.
7. Springmann, M.; Clark, M.; Mason-D'Croz, D.; Wiebe, K.; Bodirsky, B.L.; Lassaletta, L.; de Vries, W.; Vermeulen, S.J.; Herrero, M.; Carlson, K.M. Options for keeping the food system within environmental limits. *Nature* **2018**, *562*, 519. [CrossRef]
8. Kah, M.; Kookana, R.S.; Gogos, A.; Bucheli, T.D. A critical evaluation of nanopesticides and nanofertilizers against their conventional analogues. *Nat. Nanotechnol.* **2018**, *13*, 677. [CrossRef]
9. Clark, M.; Tilman, D. Comparative analysis of environmental impacts of agricultural production systems, agricultural input efficiency, and food choice. *Environ. Res. Lett.* **2017**, *12*, 064016. [CrossRef]
10. Guo, T.; Johnson, L.T.; LaBarge, G.A.; Penn, C.J.; Stumpf, R.P.; Baker, D.B.; Shao, G. Less Agricultural Phosphorus Applied in 2019 Led to Less Dissolved Phosphorus Transported to Lake Erie. *Environ. Sci. Technol.* **2021**, *55*, 283–291. [CrossRef] [PubMed]
11. Saia, S.M.; Carrick, H.J.; Buda, A.R.; Regan, J.M.; Walter, M.T. Critical Review of Polyphosphate and Polyphosphate Accumulating Organisms for Agricultural Water Quality Management. *Environ. Sci. Technol.* **2021**, *55*, 2722–2742. [CrossRef]
12. Ceulemans, T.; Bodé, S.; Bollyn, J.; Harpole, S.; Coorevits, K.; Peeters, G.; Van Acker, K.; Smolders, E.; Boeckx, P.; Honnay, O. Phosphorus resource partitioning shapes phosphorus acquisition and plant species abundance in grasslands. *Nat. Plants* **2017**, *3*, 1–7. [CrossRef] [PubMed]
13. Hawkesford, M.J.; Kopriva, S.; De Kok, L.J. *Nutrient Use Efficiency in Plants*; Springer: Berlin/Heidelberg, Germany, 2016.
14. Dobermann, A. Nutrient use efficiency–measurement and management. In *Fertilizer Best Management Practices*; IFA: Paris, France, 2007.
15. Wang, J.; Bouwman, A.F.; Liu, X.; Beusen, A.H.; Van Dingenen, R.; Dentener, F.; Yao, Y.; Glibert, P.M.; Ran, X.; Yao, Q. Harmful Algal Blooms in Chinese Coastal Waters Will Persist Due to Perturbed Nutrient Ratios. *Environ. Sci. Technol. Lett.* **2021**, *8*, 276–284. [CrossRef]
16. Némery, J.; Garnier, J. The fate of phosphorus. *Nat. Geosci.* **2016**, *9*, 343–344. [CrossRef]
17. Vaccari, D.A.; Powers, S.M.; Liu, X. Demand-driven model for global phosphate rock suggests paths for phosphorus sustainability. *Environ. Sci. Technol.* **2019**, *53*, 10417–10425. [CrossRef]
18. Liu, W.; Ciais, P.; Liu, X.; Yang, H.; Hoekstra, A.Y.; Tang, Q.; Wang, X.; Li, X.; Cheng, L. Global Phosphorus Losses from Croplands under Future Precipitation Scenarios. *Environ. Sci. Technol.* **2020**, *54*, 14761–14771. [CrossRef]
19. Alewell, C.; Ringeval, B.; Ballabio, C.; Robinson, D.A.; Panagos, P.; Borrelli, P. Global phosphorus shortage will be aggravated by soil erosion. *Nat. Commun.* **2020**, *11*, 1–12. [CrossRef] [PubMed]
20. Hofmann, T.; Lowry, G.V.; Ghoshal, S.; Tufenkji, N.; Brambilla, D.; Dutcher, J.R.; Gilbertson, L.M.; Giraldo, J.P.; Kinsella, J.M.; Landry, M.P. Technology readiness and overcoming barriers to sustainably implement nanotechnology-enabled plant agriculture. *Nat. Food* **2020**, *1*, 416–425. [CrossRef]

21. Johnston, A.E.; Poulton, P.R.; Fixen, P.E.; Curtin, D. Phosphorus: Its efficient use in agriculture. In *Advances in Agronomy*; Elsevier: Amsterdam, The Netherlands, 2014; Volume 123, pp. 177–228.
22. Group, A.C. Innovative Approach Taken to Phosphorus Nanofertilizer Research. Available online: https://www.agchemigroup.eu/en/blog/post/innovative-approach-taken-phosphorus-nanofertilizer-research (accessed on 24 May 2018).
23. Lowry, G.V.; Avellan, A.; Gilbertson, L.M. Opportunities and challenges for nanotechnology in the agri-tech revolution. *Nat. Nanotechnol.* **2019**, *14*, 517–522. [CrossRef] [PubMed]
24. Yin, J.; Wang, Y.; Gilbertson, L.M. Opportunities to advance sustainable design of nano-enabled agriculture identified through a literature review. *Environ. Sci. Nano* **2018**, *5*, 11–26. [CrossRef]
25. Vázquez-Núñez, E.; López-Moreno, M.L.; de la Rosa Álvarez, G.; Fernández-Luqueño, F. Incorporation of Nanoparticles into Plant Nutrients: The Real Benefits. In *Agricultural Nanobiotechnology*; Springer: Berlin/Heidelberg, Germany, 2018; pp. 49–76.
26. Subramanian, K.S.; Manikandan, A.; Thirunavukkarasu, M.; Rahale, C.S. Nano-fertilizers for balanced crop nutrition. In *Nanotechnologies in Food and Agriculture*; Springer: Berlin/Heidelberg, Germany, 2015; pp. 69–80.
27. Raliya, R.; Saharan, V.; Dimkpa, C.; Biswas, P. Nanofertilizer for precision and sustainable agriculture: Current state and future perspectives. *J. Agric. Food. Chem.* **2017**, *66*, 6487–6503. [CrossRef]
28. Dimkpa, C.O.; Bindraban, P.S. Nanofertilizers: New products for the industry? *J. Agric. Food. Chem.* **2017**, *66*, 6462–6473. [CrossRef] [PubMed]
29. Zhao, L.; Huang, Y.; Keller, A.A. Comparative metabolic response between cucumber (Cucumis sativus) and corn (Zea mays) to a Cu (OH) 2 nanopesticide. *J. Agric. Food. Chem.* **2017**, *66*, 6628–6636. [CrossRef]
30. Chariou, P.L.; Ortega-Rivera, O.A.; Steinmetz, N.F. Nanocarriers for the Delivery of Medical, Veterinary, and Agricultural Active Ingredients. *ACS Nano* **2020**, *14*, 2678–2701. [CrossRef]
31. Talreja, N.; Chauhan, D.; Rodríguez, C.A.; Mera, A.C.; Ashfaq, M. Nanocarriers: An Emerging Tool for Micronutrient Delivery in Plants. In *Plant Micronutrients*; Springer: Berlin/Heidelberg, Germany, 2020; pp. 373–387.
32. Lew, T.T.S.; Koman, V.B.; Silmore, K.S.; Seo, J.S.; Gordiichuk, P.; Kwak, S.-Y.; Park, M.; Ang, M.C.-Y.; Khong, D.T.; Lee, M.A. Real-time detection of wound-induced H 2 O 2 signalling waves in plants with optical nanosensors. *Nat. Plants* **2020**, *6*, 404–415. [CrossRef]
33. Kashyap, P.L.; Kumar, S.; Jasrotia, P.; Singh, D.; Singh, G.P. Nanosensors for plant disease diagnosis: Current understanding and future perspectives. In *Nanoscience for Sustainable Agriculture*; Springer: Berlin/Heidelberg, Germany, 2019; pp. 189–205.
34. Srivastava, A.K.; Dev, A.; Karmakar, S. Nanosensors and nanobiosensors in food and agriculture. *Environ. Chem. Lett.* **2018**, *16*, 161–182. [CrossRef]
35. Gilbertson, L.M.; Pourzahedi, L.; Laughton, S.; Gao, X.; Zimmerman, J.B.; Theis, T.L.; Westerhoff, P.; Lowry, G.V. Guiding the design space for nanotechnology to advance sustainable crop production. *Nat. Nanotechnol.* **2020**, *15*, 801–810. [CrossRef]
36. Ditta, A.; Mehmood, S.; Imtiaz, M.; Rizwan, M.S.; Islam, I. Soil fertility and nutrient management with the help of nanotechnology. In *Nanomaterials for Agriculture and Forestry Applications*; Elsevier: Amsterdam, The Netherlands, 2020; pp. 273–287.
37. Liu, B.; Fan, Y.; Li, H.; Zhao, W.; Luo, S.; Wang, H.; Guan, B.; Li, Q.; Yue, J.; Dong, Z. Control the entire journey of pesticide application on superhydrophobic plant surface by dynamic covalent trimeric surfactant coacervation. *Adv. Funct. Mater.* **2021**, *31*, 2006606. [CrossRef]
38. Liu, R.; Lal, R. Synthetic apatite nanoparticles as a phosphorus fertilizer for soybean (*Glycine max*). *Sci. Rep.* **2014**, *4*, 5686. [CrossRef] [PubMed]
39. Wu, L.; Liu, M. Preparation and properties of chitosan-coated NPK compound fertilizer with controlled-release and water-retention. *Carbohydr. Polym.* **2008**, *72*, 240–247. [CrossRef]
40. Tang, S.; Fei, X. Refractory Calcium Phosphate-Derived Phosphorus Fertilizer Based on Hydroxyapatite Nanoparticles for Nutrient Delivery. *ACS Appl. Nano Mater.* **2021**, *4*, 1364–1376. [CrossRef]
41. Soliman, A.S.; Hassan, M.; Abou-Elella, F.; Ahmed, A.H.; El-Feky, S.A. Effect of nano and molecular phosphorus fertilizers on growth and chemical composition of baobab (*Adansonia digitata* L.). *J. Plant Sci.* **2016**, *11*, 52–60. [CrossRef]
42. Ma, C.; Borgatta, J.; De La Torre Roche, R.; Zuverza-Mena, N.; White, J.C.; Hamers, R.J.; Elmer, W. Time-dependent transcriptional response of tomato (*Solanum lycopersicum* L.) to Cu nanoparticle exposure upon infection with *Fusarium oxysporum* f. sp. lycopersici. *ACS Sustain. Chem. Eng.* **2019**, *7*, 10064–10074. [CrossRef]
43. Ali, S.; Rizwan, M.; Noureen, S.; Anwar, S.; Ali, B.; Naveed, M.; Abd_Allah, E.F.; Alqarawi, A.A.; Ahmad, P. Combined use of biochar and zinc oxide nanoparticle foliar spray improved the plant growth and decreased the cadmium accumulation in rice (*Oryza sativa* L.) plant. *Environ. Sci. Pollut. Res.* **2019**, *26*, 11288–11299. [CrossRef]
44. Rui, M.; Ma, C.; Hao, Y.; Guo, J.; Rui, Y.; Tang, X.; Zhao, Q.; Fan, X.; Zhang, Z.; Hou, T. Iron oxide nanoparticles as a potential iron fertilizer for peanut (*Arachis hypogaea*). *Front. Plant Sci.* **2016**, *7*, 815. [CrossRef]
45. Pradhan, S.; Patra, P.; Das, S.; Chandra, S.; Mitra, S.; Dey, K.K.; Akbar, S.; Palit, P.; Goswami, A. Photochemical modulation of biosafe manganese nanoparticles on Vigna radiata: A detailed molecular, biochemical, and biophysical study. *Environ. Sci. Technol.* **2013**, *47*, 13122–13131. [CrossRef] [PubMed]
46. Jassby, D.; Su, Y.; Kim, C.; Ashworth, V.; Adeleye, A.S.; Rolshausen, P.; Roper, C.; White, J. Delivery, Uptake, Fate, and Transport of Engineered Nanoparticles in Plants: A Critical Review and Data Analysis. *Environ. Sci. Nano* **2019**, *6*, 2311–2331.
47. Carnovale, C.; Bryant, G.; Shukla, R.; Bansal, V. Identifying Trends in Gold Nanoparticle Toxicity and Uptake: Size, Shape, Capping Ligand, and Biological Corona. *ACS Omega* **2019**, *4*, 242–256. [CrossRef]

48. Raliya, R.; Franke, C.; Chavalmane, S.; Nair, R.; Reed, N.; Biswas, P. Quantitative understanding of nanoparticle uptake in watermelon plants. *Front. Plant Sci.* **2016**, *7*, 1288. [CrossRef] [PubMed]
49. Zhu, Z.-J.; Wang, H.; Yan, B.; Zheng, H.; Jiang, Y.; Miranda, O.R.; Rotello, V.M.; Xing, B.; Vachet, R.W. Effect of surface charge on the uptake and distribution of gold nanoparticles in four plant species. *Environ. Sci. Technol.* **2012**, *46*, 12391–12398. [CrossRef]
50. Spielman-Sun, E.; Avellan, A.; Bland, G.D.; Tappero, R.V.; Acerbo, A.S.; Unrine, J.M.; Giraldo, J.P.; Lowry, G.V. Nanoparticle surface charge influences translocation and leaf distribution in vascular plants with contrasting anatomy. *Environ. Sci. Nano* **2019**, *6*, 2508–2519. [CrossRef]
51. Wang, D.; Jin, Y.; Jaisi, D.P. Effect of size-selective retention on the cotransport of hydroxyapatite and goethite nanoparticles in saturated porous media. *Environ. Sci. Technol.* **2015**, *49*, 8461–8470. [CrossRef]
52. Ditta, A. How helpful is nanotechnology in agriculture? *Adv. Nat. Sci. Nanosci. Nanotechnol.* **2012**, *3*, 033002. [CrossRef]
53. Zhou, H.; Lee, J. Nanoscale hydroxyapatite particles for bone tissue engineering. *Acta Biomater.* **2011**, *7*, 2769–2781. [CrossRef] [PubMed]
54. Palazzo, B.; Iafisco, M.; Laforgia, M.; Margiotta, N.; Natile, G.; Bianchi, C.L.; Walsh, D.; Mann, S.; Roveri, N. Biomimetic hydroxyapatite–drug nanocrystals as potential bone substitutes with antitumor drug delivery properties. *Adv. Funct. Mater.* **2007**, *17*, 2180–2188. [CrossRef]
55. Xiong, L.; Wang, P.; Kopittke, P.M. Tailoring hydroxyapatite nanoparticles to increase their efficiency as phosphorus fertilisers in soils. *Geoderma* **2018**, *323*, 116–125. [CrossRef]
56. Sadat-Shojai, M.; Khorasani, M.-T.; Dinpanah-Khoshdargi, E.; Jamshidi, A. Synthesis methods for nanosized hydroxyapatite with diverse structures. *Acta Biomater.* **2013**, *9*, 7591–7621. [CrossRef]
57. Loo, S.C.J.; Siew, Y.E.; Ho, S.; Boey, F.Y.C.; Ma, J. Synthesis and hydrothermal treatment of nanostructured hydroxyapatite of controllable sizes. *J. Mater. Sci. Mater. Med.* **2008**, *19*, 1389–1397. [CrossRef]
58. Xiong, L.; Wang, P.; Hunter, M.N.; Kopittke, P.M. Bioavailability and movement of hydroxyapatite nanoparticles (HA-NPs) applied as a phosphorus fertiliser in soils. *Environ. Sci. Nano* **2018**, *5*, 2888–2898. [CrossRef]
59. Ramírez-Rodríguez, G.B.; Dal Sasso, G.; Carmona, F.J.; Miguel-Rojas, C.; Pérez-de-Luque, A.; Masciocchi, N.; Guagliardi, A.; Delgado-López, J.M. Engineering Biomimetic Calcium Phosphate Nanoparticles: A Green Synthesis of Slow-Release Multinutrient (NPK) Nanofertilizers. *ACS Appl. Bio Mater.* **2020**, *3*, 1344–1353. [CrossRef]
60. Yoon, H.Y.; Lee, J.G.; Esposti, L.D.; Iafisco, M.; Kim, P.J.; Shin, S.G.; Jeon, J.-R.; Adamiano, A. Synergistic release of crop nutrients and stimulants from hydroxyapatite nanoparticles functionalized with humic substances: Toward a multifunctional nanofertilizer. *ACS Omega* **2020**, *5*, 6598–6610. [CrossRef] [PubMed]
61. Rico, C.M.; Hong, J.; Morales, M.I.; Zhao, L.; Barrios, A.C.; Zhang, J.-Y.; Peralta-Videa, J.R.; Gardea-Torresdey, J.L. Effect of cerium oxide nanoparticles on rice: A study involving the antioxidant defense system and in vivo fluorescence imaging. *Environ. Sci. Technol.* **2013**, *47*, 5635–5642. [CrossRef] [PubMed]
62. Navarro, D.A.; Bisson, M.A.; Aga, D.S. Investigating uptake of water-dispersible CdSe/ZnS quantum dot nanoparticles by Arabidopsis thaliana plants. *J. Hazard. Mater.* **2012**, *211*, 427–435. [CrossRef] [PubMed]
63. Chen, G.; Ma, C.; Mukherjee, A.; Musante, C.; Zhang, J.; White, J.C.; Dhankher, O.P.; Xing, B. Tannic acid alleviates bulk and nanoparticle Nd2O3 toxicity in pumpkin: A physiological and molecular response. *Nanotoxicology* **2016**, *10*, 1243–1253. [CrossRef] [PubMed]
64. Lichtenthaler, H.K.; Buschmann, C. Chlorophylls and carotenoids: Measurement and characterization by UV-VIS spectroscopy. *Curr. Protoc. Food Anal. Chem.* **2001**, *1*, F4.3.1–F4.3.8. [CrossRef]
65. Luna Zaragoza, D.; Romero Guzmán, E.T.; Reyes Gutiérrez, L.R. Surface and physicochemical characterization of phosphates vivianite, $Fe_2(PO_4)_3$ and hydroxyapatite, $Ca_5(PO_4)_3OH$. *J. Miner. Mater. Char. Eng.* **2009**, *8*, 591–609.
66. Koutsopoulos, S. Synthesis and characterization of hydroxyapatite crystals: A review study on the analytical methods. *J. Biomed. Mater. Res.* **2002**, *62*, 600–612. [CrossRef] [PubMed]
67. Cheng, Y.T.; Zhang, L.; He, S.Y. Plant-microbe interactions facing environmental challenge. *Cell Host Microbe* **2019**, *26*, 183–192. [CrossRef]
68. Chen, T.; Nomura, K.; Wang, X.; Sohrabi, R.; Xu, J.; Yao, L.; Paasch, B.C.; Ma, L.; Kremer, J.; Cheng, Y. A plant genetic network for preventing dysbiosis in the phyllosphere. *Nature* **2020**, *580*, 653–657. [CrossRef]
69. Xiang, Q.; Lott, A.A.; Assmann, S.M.; Chen, S. Advances and perspectives in the metabolomics of stomatal movement and the disease triangle. *Plant Sci.* **2020**, 110697.
70. Unger, P.W.; Kaspar, T.C. Soil compaction and root growth: A review. *Agron. J.* **1994**, *86*, 759–766. [CrossRef]
71. Guidi, L.; Degl'Innocenti, E. Imaging of chlorophyll a fluorescence: A tool to study abiotic stress in plants. In *Abiotic Stress Plants—Mechanisms and Adaptions*; InTech: Rijeka, Croatia, 2011.
72. Guidi, L.; Lo Piccolo, E.; Landi, M. Chlorophyll fluorescence, photoinhibition and abiotic stress: Does it make any difference the fact to be a C3 or C4 species? *Front. Plant Sci.* **2019**, *10*, 174. [CrossRef] [PubMed]
73. Kalaji, M.H.; Goltsev, V.N.; Żuk-Gołaszewska, K.; Zivcak, M.; Brestic, M. *Chlorophyll Fluorescence: Understanding Crop Performance—Basics and Applications*; CRC Press: Boca Raton, FL, USA, 2017.
74. Carstensen, A.; Szameitat, A.E.; Frydenvang, J.; Husted, S. Chlorophyll a fluorescence analysis can detect phosphorus deficiency under field conditions and is an effective tool to prevent grain yield reductions in spring barley (*Hordeum vulgare* L.). *Plant Soil* **2019**, *434*, 79–91. [CrossRef]

75. Hepler, P.K. Calcium: A central regulator of plant growth and development. *Plant Cell* **2005**, *17*, 2142–2155. [CrossRef]
76. de Bang, T.C.; Husted, S.; Laursen, K.H.; Persson, D.P.; Schjoerring, J.K. The molecular–physiological functions of mineral macronutrients and their consequences for deficiency symptoms in plants. *New Phytol.* **2021**, *229*, 2446–2469. [CrossRef] [PubMed]
77. Ma, J.; Ma, Y.; Wei, R.; Chen, Y.; Weng, L.; Ouyang, X.; Li, Y. Phosphorus transport in different soil types and the contribution of control factors to phosphorus retardation. *Chemosphere* **2021**, *276*, 130012. [CrossRef]
78. Gérard, F. Clay minerals, iron/aluminum oxides, and their contribution to phosphate sorption in soils—A myth revisited. *Geoderma* **2016**, *262*, 213–226. [CrossRef]
79. Mayakaduwage, S.; Mosley, L.M.; Marschner, P. Threshold for labile phosphate in a sandy acid sulfate soil. *Geoderma* **2020**, *371*, 114359. [CrossRef]
80. Fernández, V.; Eichert, T. Uptake of hydrophilic solutes through plant leaves: Current state of knowledge and perspectives of foliar fertilization. *Crit. Rev. Plant Sci.* **2009**, *28*, 36–68. [CrossRef]
81. Nair, R.; Varghese, S.H.; Nair, B.G.; Maekawa, T.; Yoshida, Y.; Kumar, D.S. Nanoparticulate material delivery to plants. *Plant Sci.* **2010**, *179*, 154–163. [CrossRef]
82. Droux, M. Sulfur assimilation and the role of sulfur in plant metabolism: A survey. *Photosynth. Res.* **2004**, *79*, 331–348. [CrossRef]
83. Wilhelm Scherer, H. Sulfur in soils. *J. Plant Nutr. Soil Sci.* **2009**, *172*, 326–335. [CrossRef]
84. Prodhan, M.A.; Finnegan, P.M.; Lambers, H. How does evolution in phosphorus-impoverished landscapes impact plant nitrogen and sulfur assimilation? *Trends Plant Sci.* **2019**, *24*, 69–82. [CrossRef]
85. Veneklaas, E.J.; Lambers, H.; Bragg, J.; Finnegan, P.M.; Lovelock, C.E.; Plaxton, W.C.; Price, C.A.; Scheible, W.R.; Shane, M.W.; White, P.J. Opportunities for improving phosphorus-use efficiency in crop plants. *New Phytol.* **2012**, *195*, 306–320. [CrossRef]
86. Singh, S.K.; Reddy, V.R.; Fleisher, D.H.; Timlin, D.J. Phosphorus nutrition affects temperature response of soybean growth and canopy photosynthesis. *Front. Plant Sci.* **2018**, *9*, 1116. [CrossRef]
87. Priester, J.H.; Ge, Y.; Mielke, R.E.; Horst, A.M.; Moritz, S.C.; Espinosa, K.; Gelb, J.; Walker, S.L.; Nisbet, R.M.; An, Y.-J. Soybean susceptibility to manufactured nanomaterials with evidence for food quality and soil fertility interruption. *Proc. Natl. Acad. Sci. USA* **2012**, *109*, E2451–E2456. [CrossRef] [PubMed]
88. Bishnoi, U.R.; Kaur, G.; Khan, M. Calcium, phosphorus, and harvest stages effects soybean seed production and quality. *J. Plant Nutr.* **2007**, *30*, 2119–2127. [CrossRef]